Hindawi
Journal of Combustion
Volume 2021, Article ID 6673494, 11 pages
https://doi.org/10.1155/2021/6673494

Research Article

Multiphysical Models for Hydrogen Production Using NaOH and Stainless Steel Electrodes in Alkaline Electrolysis Cell

Ivan Newen Aquigeh, Merlin Zacharie Ayissi, and Dieudonné Bitondo

Ecole National Supérieure Polytechnique de Douala Laboratory,
Energy, Materials, Modelling and Methods (E3M) University of Douala, Douala, Cameroon

Correspondence should be addressed to Ivan Newen Aquigeh; ivannewen@yahoo.com

Received 28 October 2020; Revised 24 February 2021; Accepted 11 March 2021; Published 20 March 2021

Academic Editor: Siamak Hoseinzadeh

The cell voltage in alkaline water electrolysis cells remains high despite the fact that water electrolysis is a cleaner and simpler method of hydrogen production. A multiphysical model for the cell voltage of a single cell electrolyzer was realized based on a combination of current-voltage models, simulation of electrolyzers in intermittent operation (SIMELINT), existing experimental data, and data from the experiment conducted in the course of this work. The equipment used NaOH as supporting electrolyte and stainless steel as electrodes. Different electrolyte concentrations, interelectrode gaps, and electrolyte types were applied and the cell voltages recorded. Concentrations of 60 wt% NaOH produced lowest range of cell voltage (1.15–2.67 V); an interelectrode gap of 0.5 cm also presented the lowest cell voltage (1.14–2.71 V). The distilled water from air conditioning led to a minimum cell voltage (1.18–2.78 V). The water from a factory presented the highest flow rate (12.48×10^{-1} cm^3/min). It was found that the cell voltage of the alkaline electrolyzer was reduced considerably by reducing the interelectrode gap to 0.5 cm and using electrolytes that produce less bubbles. A maximum error of 1.5% was found between the mathematical model and experimental model, indicating that the model is reliable.

1. Introduction

The continuous use of fossil fuels and biofuels due to high energy demands poses problems of pollution, feedstock, and quality challenges [1–3]. The production and application of hydrogen still remains expensive and the technology is still premature [4, 5]. Furthermore, it is a high energy-consuming technology. In fact, 2393 Ah are required to produce 1 Nm^3 of hydrogen [6]. The transportation sector still encounters the problem of space and load for tanks and storage batteries for the FCEVs [7], therefore the need to produce on the spot for consumption, giving credit to the continuous research in alkaline water electrolysis (AWE).

Combustion of fossil fuels and their overuse lead to severe air pollution, global warming, acid rains, and ozone depletion in stratosphere [8–10]. The search for possible alternative sources of energy is a must. There are a number of primary energy sources available, such as thermonuclear energy, solar energy, wind energy, hydropower, and geothermal energy. Unfortunately, they cannot be used directly like fossil fuels. In most cases, they need to be converted into fuels leading to a search for a new energy carrier [11]. Hydrogen fuel cells are two to three times more efficient than combustion engines [12]. They are becoming more widely available and would reduce the dependency on fossil fuels. In a fuel cell, hydrogen and oxygen are combined in an electrochemical reaction that produces electricity and a byproduct: water. The production of hydrogen for fuel cell applications requires performance improvements. In spite of considerable achievement realized so far in the field of polymer electrolyte membrane fuel cells, one substantial question has not been answered yet; i.e., what combination of performance criteria brings the greatest benefits? [13, 14].

Currently, the supply and use of energy from fossil fuels is unsustainable economically, environmentally, and socially. Without decisive action, energy-related emissions of carbon dioxide (CO_2) will be more than double by 2050

[6, 12, 15] and increased fossil energy demand will heighten concerns over the security of supply [3]. The current path can and must be changed [12]. This calls for an energy revolution and low-carbon energy technologies to play a crucial role [16]. Hydrogen technologies are already commercially available [17]. One of the technologies is thermo catalytic and gasification processes using natural gas as a starting material, and heavy oils and naphtha make up the next largest source, followed by coal. About half of the hydrogen produced is obtained through these technologies [1, 2, 8], which are neither renewable nor clean. They involve carbon capture and storage, leading to their reduced efficiency. Autothermal processes suffer from high energy requirements and high startup time [18]. Biohydrogen production is inexpensive and favors waste management but employs expensive raw materials in some cases. Furthermore, low rates and yields of hydrogen formation are achieved and the technology is at the experimental level in the laboratory. Alkaline electrolyzers are currently the most mature technology, and investment costs are considerably lower than for others [12, 19–22]. Production of hydrogen by water electrolysis is very low (<4%) [23]. However, water electrolysis yields clean hydrogen in small amounts. Unexpectedly, at a larger scale, production of hydrogen is expensive. Recent research studies for hydrogen production improvement employed pressurized water electrolysis, others use plasma technology, and today natural hydrogen sources do exist. Pressurized water electrolysis presents high rate of gas crossover [24]. With the plasma technology, more hydrogen is produced at lower concentrations of NH_3 but under high temperatures, increased energy cost, and unwanted cooking and soot [17]. Concerning natural hydrogen, little is known about its generation, migration, consumption, and potential accumulation [5, 25].

Electrolyzer models are generally formulated with Faraday's law [4, 26]. Empirical models describing the electrolysis process developed by Ulleberg [27] and modified by Hug et al. [28] are widely used to evaluate the characteristics of cell performance. Electrodes made of different materials were used as well as different electrolyte concentrations, membranes of different materials, different types of electrolytes, and a variety of cell geometrical, and physicochemical parameters [29]. Models from first principles have been developed with theoretical considerations made on the basis of the theories of Laplace, Newton–Raphson, and Dirichlet to express the most significant parameters influencing the operation of monopolar or bipolar electrochemical reactors (current-potential distribution) [30, 31]. Algorithms capable of helping designers develop more efficient electrochemical reactors were derived enabling the calculation of current-potential distributions [30]. Slama [32] and Rashed and Elmaihy [33] found that there is a significant increase of hydrogen production flow by the use of additives such as NaCl, KOH, and NaOH. KOH has a higher ionic conductivity compared to NaOH [34]. KOH is highly corrosive, limiting the type of materials to be used in the AWEs. Nickel is relatively cheaper and less corrosive, so it is suitable to be used with KOH [34–36]. Tijani et al. [4] and Martinez and Zamora [37], using MATLAB, simulated a mathematical model for the cell voltage with limited facts as compared to the model of Diaz [38] who used MATLAB/Simulink. The model of Tijani et al. [4] does not take into account the effects of pressure, concentration, bubbles, and volumetric vacuum which are considered in the model of Camilo [38]. Baseline experiments using platinum electrodes and KOH as electrolyte additive have been carried out indicating that interelectrode gap, electrolyte concentrations, and electrolyte type are the most significant parameters affecting cell performance [39].

In this paper, the ideas of Opu [39], Tijani et al. [4], and Diaz [38] have been combined to come out with multiphysical models using NaOH as supporting electrolyte instead of KOH and stainless steel electrodes instead of noble metals like platinum. In the quest of reducing the energy consumed per Nm^3 of hydrogen produced and improving the flow rate in order to produce cost effective hydrogen, the cell performances for different levels of three independent variables were experimented. The above mentioned variables included (i) electrolyte concentration, (ii) electrolyte type, and (iii) interelectrode gap. Investigations on the flow rate for different electrolyte types were done by recording the time to 1000 ppm and calculating the hydrogen flow rate. These were done by performing experiments, executing in MATLAB, and in combination with existing models and existing parameters in the literature, a multiphysical model was established for the cell voltage of an electrolyzer. This paper aims to investigate the interelectrode gap, the electrolyte concentration, and the types of electrolyte that can affect the production of hydrogen.

2. Materials and Methods

Self-working temperatures as a result of the addition of NaOH are considered constant as we took measurements each time the temperatures were around 80°C. The experiment was designed such that each experiment considered a single independent variable with three levels each and the results are compared to the baseline experiment. Since the design considered one independent variable per experiment, 10 trials per level were done and the means calculated.

2.1. Existing Models. Polarization curves were produced to characterize the process. Existing current-voltage (I-V) models have been used for the simulations as formulated by Tijani et al. [4] and Ulleberg [27]:

$$V_{\text{cell}} = V_{\text{rev}} + V_{\text{ohm}} + V_{\text{act}}, \tag{1}$$

where V_{cell} is the cell voltage, V_{rev} is the reversible voltage, V_{ohm} is the ohmic voltage, and V_{act} is the activation voltage.

$$V_{\text{ohm}} = \frac{r_1 + r_2 T}{A} I, \tag{2}$$

where T is the temperature of the cell, A is the area of the electrodes, and r_1 and r_2 are the ohmic overvoltage parameters.

$$V_{\text{act}} = s\log\left(t_1 + (t_2/T) + \left(\frac{t_3/T^2)}{A\,I + 1}\right)\right), \tag{3}$$

where t_1, t_2, t_3, and s are the activation overvoltage parameters.

The reversible voltage (V_{rev}) is the minimum electric voltage that must be applied to both electrodes to enable the electrochemical reaction. It is a constant value of approximately 1.229 V obtained from the Gibbs relation [4]:

$$V_{\text{rev}} = \frac{\Delta G}{ZF}, \tag{4}$$

where ΔG is the Gibbs energy, Z is the number of electrons, and F is the Faraday constant.

The ohmic overvoltage (V_{ohm}) is as a result of electrochemical resistance due to the presence of bubbles in the electrolyte, ionic resistivity of the electrolyte, interelectrode gap, membrane (diaphragm) resistivity, electrolyte concentration, temperature effects, type of electrolyte, and other phenomena. The activation voltage is as a result of resistance from the electrode material type, electrode dimension, electrode shape, electrode operating temperature, and other aspects related to the electrodes. V_{ohm} and V_{act} are temperature dependent and take into account the ohmic resistance parameter, r, and the overpotential coefficients s and t, as suggested by Ulleberg [27].

The data used in the above modelling is shown in Table 1; constant parameters used for simulation calculations are given.

Hug et al. [28] have developed a model to analyse the performance of an electrolyzer, which expressed the cell voltage as follows:

$$V_{\text{cell}} = E_{\text{rev}} + A_1 + A_2\log(i), \tag{5}$$

where E_{rev} is the theoretical voltage, A_1 is the ohmic loss, and $A_2\log(i)$ is the activation overpotential. Diaz [38] used KOH as the electrolyte and came out with the following model:

$$\begin{aligned} V_{\text{cell}(T,P,C,J)} &= E_{\text{th}(T,P,C)} \\ &\quad + b_c\cdot\log\left(\frac{J_{\text{eff}-c}}{J_{o-c}}\right) + b_a\cdot\log\left(\frac{J_{\text{eff}-a}}{J_{o-a}}\right) \\ &\quad + \left[R_{\text{cat}} + R_{\text{ano}} + R_{\text{mem}} + R_{\text{KOH}-\varepsilon}\right]i, \end{aligned} \tag{6}$$

$$\left[R_{\text{cat}} + R_{\text{ano}} + R_{\text{mem}} + R_{\text{KOH}-\varepsilon}\right] = R_T, \tag{7}$$

where $E_{\text{th}(T,P,C)}$ is the theoretical voltage and is a constant (−1.229 V); b_c and b_a are Tafel's coefficients for the cathode and anode, respectively; $J_{\text{eff}-c}$ and $J_{\text{eff}-a}$ are the effective current densities of the cathode and anode, respectively; J_{o-c} and J_{o-a} are the exchange current densities of the cathode and anode, respectively; R_T is the total resistance; i is the electrolyzer's current;R_{cat} is the resistance of the cathode; R_{ano} is the resistance of the anode; R_{mem} is the resistance of the membrane; and $R_{\text{KOH}-\varepsilon}$ is the resistance of the electrolyte with bubbles considered [34].

On the basis of the high sensitivity of the gas detector used in this work, the hydrogen gas detector was used to determine the flow rate, by setting the detector and recording the time taken to attain 1000 ppm and this time is used to calculate the flow rate. From the physical relation below, the concentration is converted to a volume fraction of hydrogen developed by Never [40], Godish [41], and Cohen and Taylor [42].

$$\begin{aligned} 1\text{ ppm} &= \frac{1\,\mu\text{L gas}}{1\text{ L air}} = \frac{V_m}{M}\,\frac{1\,\mu\text{g gas}}{1\text{ L air}} = \frac{1\,\mu\text{ mole gas}}{1\text{ mole air}}, \\ 1000\text{ ppm} &= \frac{1000\,\mu\text{ mole H}_2}{1\text{ mole air}} = \frac{1000\,\mu\text{L gas}}{1\text{ L air}} = \frac{10^{-6}\text{m}^3\text{ gas}}{1\text{ L air}}, \end{aligned} \tag{8}$$

where V_m is the standard molar volume of ideal gas (22.71108 L/mol) and M is the molar weight of gas.

The current or Faraday efficiency is an important tool to determine the specific energy consumption of an electrolyzer, particularly at partial load [28]. It is obtained from the following relationships, established by Tijani et al. [4], Rashid et al. [21], Schalenbach et al. [24], and Chisholm and Cronin [43]:

$$\eta_c = \frac{\eta_{\text{cell}}}{\eta_u}, \tag{9}$$

where η_c is the current efficiency, η_{cell} is the cell efficiency, and η_u is the voltage efficiency.

$$\begin{aligned} \eta_{\text{cell}} &= \frac{\text{moles of hydrogen}\times \text{HHV}_{\text{H}_2}}{I\times V\times t}\times 100, \\ \eta_u &= \frac{V_{\text{rev}}}{V_{\text{cell}}}. \end{aligned} \tag{10}$$

2.2. Experimental Setup. Various instruments were used in the experiment (Figure 1). The diagram brings more insight on the functioning of the cell (Figure 2).

2.2.1. Constituents of the Experimental Setup. The baseline experimental electrolyzer was constructed with 200 ml 40 w % sodium hydroxide (NaOH) electrolyte. Each electrode was made up of a 10 cm long, 4 mm diameter straight stainless steel rod, with a 3 cm length submerged in NaOH solution. The electrodes were kept 1 cm apart for the baseline. The electrodes were connected to a DC power supply (Model PS-305D) manufactured by Guangzhou Xinyue Electronic Technology Co., Ltd., Guangzhou, China (Table 2). The effective surface area of the electrode in the electrolyte was calculated to be about 0.38957 cm^2.

During the testing, a digital thermometer was used to monitor the temperature of the electrolyte. A hydrogen detector (S311) manufactured by Zhongan Electronic Detection Technology Co., Ltd., Zhengzhou, China (Table 3) was used to detect the presence of hydrogen during the experiments and also permitted the calculation of the flow rate.

Table 1: Parameters used by Tijani et al. [4].

Symbol	Description	Value	Units
V_{rev}	Reversible voltage	1.229	V
F	Faraday's constant	96485	C/mol
A	Electrode area	0.25	m^2
Z	Number of electrons	2	—
s	Coefficient of overvoltage on electrodes	0.185	V
t_1	Coefficient of overvoltage on electrodes	1.002	$A^{-1}m^2$
t_2	Coefficient of overvoltage on electrodes	8.424	$A^{-1}m^{2\circ}C$
t_3	Coefficient of overvoltage on electrodes	247.3	$A^{-1}m^{2\circ}C$
r_1	Parameter related to ohmic resistance of electrolyte	$8.05.e-5$	Ωm^2
r_2	Parameter related to ohmic resistance of electrolyte	$2.5.e-7$	$\Omega m^{2\circ}C$

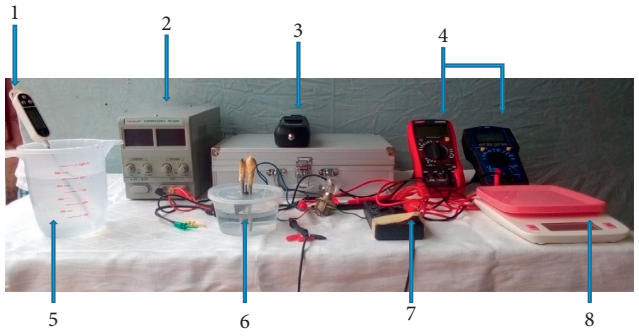

Figure 1: Elements of the experimental setup: (1) digital thermometer, (2) DC power supply, (3) hydrogen detector, (4) voltmeters, (5) plastic beaker, (6) cell, (7) ammeter, and (8.)scale balance.

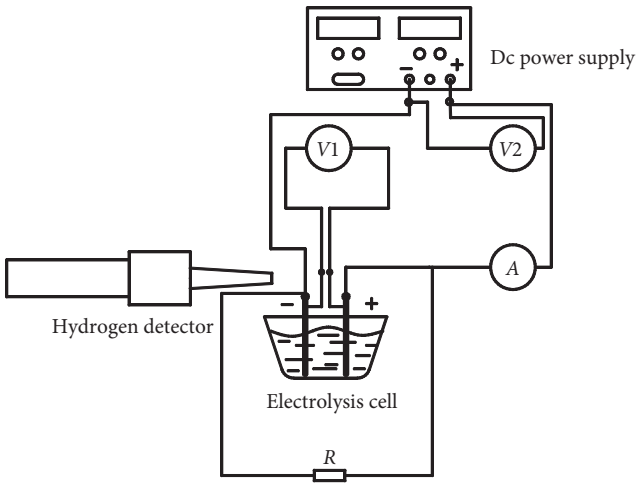

Figure 2: Diagram of experimental setup: $V1$, measuring cell voltage; $V2$, measuring supply voltage; A, measuring circuit current; R, resistor.

The detector was set at the outlet of the cathode to record the time taken to attend 1000 ppm. This information was then used to calculate the flow rate for the different liquids used.

The measuring set for cell performance was made up of three multimeters and a 12-volt bulb represented by R, connected to enable us to read the supply voltage, cell current, and cell voltages of the circuit.

Table 2: Specifications of the DC power supply.

Specifications	Technical indicators
Brand name	Yaxun
Input voltage	110/220 V
Output voltage	0 V–30 V
Output current	0–5 A
Operating temperature	−10–40°C
Relative humidity	<90%
Storage temperature	−10–70°C
Load stability	<0.2% + 3 mA
Ripple and noise	<3 mA rms
Current stability	<0.2% + 3 mA

2.2.2. Characteristics of the Electrolyte Constituents. The electrolytes used were from industrial waste (water from an air conditioning system, waste water from a dress making factory, and waste water from a dress washing machine). The physicochemical analysis of the samples was done in the HYDRAC laboratory using the standards ISO 7888 and NF T90-008 (Table 4).

3. Theory/Calculation

3.1. Multiphysical Modelling. The model considers the major aspects affecting cell performance including the following:

(i) Hydrogen bubbles around the electrodes
(ii) Ionic resistivity of the electrolyte
(iii) Oxygen bubbles
(iv) Interelectrode gap
(v) Membrane (diaphragm) resistivity
(vi) Electrode resistance
(vii) Electrolyte concentration

The model in equation (6) formulated by Diaz [38] was modified to take into account the logarithmic behaviour of cell voltages and tested with experimental parameters of KOH and NaOH, constituting the bases to the development of the multiphysical model. In fact, equation (6) was a straight line equation which when plotted could not follow a

Table 3: Specifications of the hydrogen detector.

Specifications	Technical indicator
Product model	S311
Detection principle	Electrochemistry, semiconductor or catalysis, light ion type
Sampling method	Build-in pump suction type or natural diffusion type
Response time	<30 s
Work environment	Temperature −10–55°C; relative humidity: 93% RH
Storage environment	Temperature −10–55°C
Indicating method	LCD display
Charging time	Less than 5 hours
Standby time	<8 hours
Life expectancy	2 years
Battery specifications	DC 3.7 V-1800 mAh lithium ion rechargeable battery
Weight	About 400 g
Size	255 × 70 × 51 (mm)

Table 4: Characteristics of the samples at 25°C.

Liquids	Characteristics before addition of NaOH			
	pH	Resistivity (Ωm)	Conductivity (S/m)	Salinity (g/kg)
AC water	7.65	73.153	0.0137	0.068
	>14	***0.005376***	***186.01***	***14581.5***
Water from pressing	10.67	1.7801	0.5618	3.033
	>14	***0.005144***	***194.4***	***16276.8***
Water from factory	11.21	5.0222	0.1991	1.015
	>14	***0.005297***	***188.7***	***15133.6***
Tap water	—	—	—	—
	>14	***0.00641***	***156***	***9448.6***

Values in bold italics are the characteristics after addition of 40 wt% NaOH.

logarithmic law. The modified and more realistic equation is as follows:

$$V_{\text{cell}} = V_{\text{rev}} + b_c \cdot \log\left(\frac{J_{\text{eff}-c}}{J_{o-c}}\right) + b_a \cdot \log\left(\frac{J_{\text{eff}-a}}{J_{o-a}}\right) + R_T \log(i), \tag{11}$$

where V_{rev} is the reversible overpotential and is a constant (1.229).

A generalized model for the cell performance of an alkaline electrolyzer was realized on the bases of published models and of the observations from the current experiments as well.

$$V_{\text{cell}} = KR_T \log(i) + B,$$

where: $R_T = [R_{\text{cat}} + R_{\text{ano}} + R_{\text{mem}} + R_{\text{NaOH}-\varepsilon}]$,

$$B = K\left(V_{\text{rev}} + b_c \cdot \log\left(\frac{J_{\text{eff}-c}}{J_{o-c}}\right) + b_a \cdot \log\left(\frac{J_{\text{eff}-a}}{J_{o-a}}\right)\right) + L. \tag{12}$$

Therefore,

$$V_{\text{cell}} = K\left[(R_{\text{cat}} + R_{\text{ano}} + R_{\text{mem}} + R_{\text{NaOH}-\varepsilon})\log(i) + \left(V_{\text{rev}} + b_c \cdot \log\left(\frac{J_{\text{eff}-c}}{J_{o-c}}\right) + b_a \cdot \log\left(\frac{J_{\text{eff}-a}}{J_{o-a}}\right)\right)\right] + L,$$

$$R_{\text{NaOH}-\varepsilon} = R_{\text{NaOH}}\left(\frac{1}{(1-\varepsilon)^{(3/2)}}\right), \tag{13}$$

where R_{NaOH} is the resistance of sodium hydroxide and ε is the gas void fraction due to the presence of bubbles in a solution (gas void fraction or bubble coefficient).

$$R_{\text{NaOH}} = \frac{1}{\sigma_{\text{NaOH}}}\left(\frac{d_{\text{am}}}{A} + \frac{d_{\text{cm}}}{A}\right), \tag{14}$$

where σ_{NaOH} is the electrical conductivity of sodium hydroxide, d_{am} is the distance between the anode and the membrane, d_{cm} is the distance between the cathode and the membrane, and A is the area of the electrodes.

$$R_{\text{cat}} = \frac{\rho_c l_c}{A},$$
$$R_{\text{ano}} = \frac{\rho_a l_a}{A}. \quad (15)$$

$L[V]$ is a constant which depends on the parameters considered (separation distance, electrolyte concentration, and type of electrolyte values); it is a negative voltage due to the reactivity between the hydrogen ions and the electrode [44]. K is a correction factor, obtained from numerical trials. The other parameters are obtained from tables in literature.

3.2. Constant Parameters Used in Implementing the Models. They are the physicochemical parameters obtained from previous works for the three parameters investigated (Tables 5–7): electrolyte concentration, interelectrode gap, and electrolyte type [4, 27, 38, 45–48]. These constant parameters enabled us to come out with the models for each I-V characteristic.

4. Results and Discussion

To investigate the multiphysical effect on the energy consumed and flow rate in the production of hydrogen, experiments were designed and run. Results were expressed in the form of polarization curves and bar chart. The curves present cell performance by plotting current versus voltage. The cell voltage is an indicator of the energy consumed.

4.1. Implementation and Validation of the Multiphysical Models. The characteristic equation for the linearized curves is as follows:

$$V_i = a \log(i) + b, \quad (16)$$

where V_i is the cell voltage, i is the current, and a and b are constants.

4.1.1. Cell Performance for Different Electrolyte Concentrations. Three concentrations of NaOH were experimented, that is, 30 wt%, 50 wt%, and 60 wt%. The baseline was 40 wt% NaOH. The general way to express the performance is plot of voltage versus current. The plot showed very little variation between 30 wt% and 40 wt% NaOH and likewise 50 wt% and 60 wt% (Figure 3). The greater the concentration, the better the cell performance. In fact, a lower range of cell voltage (1.16–2.67 V) was obtained from 60 wt%, and a larger range (1.24–3.01 V) from 30 wt% NaOH. It can rightly be said that the cell performance was proportional to the electrolyte concentration. Diaz [38] found using a 24 cell electrolyzer with nickel electrodes and experimented with 15 wt%, 30 wt%, and 45 wt% KOH that 45 wt% gave an optimal result. Furthermore, Slama [32] working with 0.4 M, 0.2 M, and 0.1 M KOH had a minimum cell voltage (3.3 V) for 0.4 M concentration. This behaviour could be attributed to an increase in the electrical conductivity of the solution due to the relative high concentration of NaOH. By increasing the electrical conductivity, the electrical current flowing through the solution augmented proportionately requiring low voltage for the same current density. The ohmic resistance of water electrolysis cell is strongly dependent on the concentration of the electrolyte. High concentrations mean higher available reactant at the electrode surface area for reaction which led to an increase in hydrogen production efficiency. It was found that the conductivity and the rate of bubble build-up of solutions were concentrations-dependent. The errors calculated showed that the mathematical model and the experimental model were compatible with each other with a maximum error of 1.5% recorded at 60 wt% NaOH.

4.1.2. Cell Performance for Different Interelectrode Gaps. Three interelectrode gaps were experimented including 0.5 cm, 0.75 cm, and 2 cm. The baseline was an interelectrode gap of 1 cm. Cell voltages ranged from 1.14–2.71 V for the interelectrode gap of 0.5 cm to 1.11–3.45 V for the interelectrode gap of 2 cm (Figure 4), indicating that the closer the electrodes are, the better cell performance will be. This implied that cell performance is inversely proportional to interelectrode gap. Opu [39] using platinum electrodes and KOH as supporting electrolyte obtained cell voltages (1.25–3.12 V) and (1.25–3.75 V) for 0.5 cm and 2 cm interelectrode gaps, respectively. One of the factors affecting the resistance in the electrolysis cell is the interelectrode gap. The wider the gap, the more difficult it becomes for ions to move from one electrode to another, resulting in low performance. When the interelectrode gap is small, there is less resistance in the cell which in turn leads to an increase in the flow of electrical current and therefore improves the cell performance. The results from the experimental model are close to those of the mathematical model (maximum error equal to 0.81% for the 0.75 cm interelectrode gap).

4.1.3. Cell Performance for Different Types of Electrolyte. The three types of electrolyte included AC water, pressing water, and factory water. The tap water was the baseline for control. Cell voltage varied from 1.19–2.78 V for A.C water to 1.28–3.04 V for the control (tap water) (Figure 5). Tijani et al. [4] investigated at 80°C and 350 mA/cm^2 and found a cell voltage of 2.359 V. The voltage obtained at the same condition in this work was 2.45 V. The difference might have resulted from the parameters considered which were different from those used in the study of Tijani et al. [4]. Slama [32] using NaCl as supporting electrolyte ranked first ammonia water and urine, using the hydrogen flow rate as the cell performance indicator. It was noticed that at low current densities the cell voltage was inversely proportional to the salinity values. This could be explained by the physicochemical parameters. Furthermore, low formation of bubbles was observed. AC water presented the lowest peak (at 500 mA/cm^2) value of cell voltage 2.78 V probably due to its low propagation of bubbles. This indicated the depressive effect of bubbles in the performance of an electrolyzer. With less bubbles, the ohmic resistance is decreased resulting in a low cell voltage. Tap water presented the maximum average error of 0.77%. The clustered nature of the curves at high pH

Table 5: Parameters for the different electrolyte concentrations.

Parameters	Description	Value	Unit
V_{rev}*	Reversible voltage	1.229	V
A*	Area of electrode	0.00038	m^2
b_c,*	Tafel's coefficients for the cathode	0.195	V
b_a,*	Tafel's coefficients for the anode	0.195	V
J_{eff-c},*	Effective current density of the cathode	1500	Am^{-2}
J_{eff-a},*	Effective current density of the anode	1500	Am^{-2}
J_{o-c},*	Exchange current density of the cathode	17	Am^{-2}
J_{o-a},*	Exchange current density of the anode	17	Am^{-2}
σ_{NaOH1}	Conductivity of 40 wt% NaOH at 80°C	90.83	S/m
σ_{NaOH2}	Conductivity of 30 wt% NaOH at 70°C	84.64	S/m
σ_{NaOH3}	Conductivity of 50 wt% NaOH at 80°C	83.86	S/m
σ_{NaOH4}	Conductivity of 60 wt% NaOH at 90°C	101.25	S/m
d_{am}	Distance between the anode and the membrane	0.005	m
d_{cm}	Distance between the cathode and the membrane	0.005	m
ε_1	Void fraction of 40 wt% NaOH at 80°C	0.2	—
ε_2	Void fraction of 30 wt% NaOH at 70°C	0.24	—
ε_3	Void fraction of 50 wt% NaOH at 80°C	0.12	—
ε_4	Void fraction of 60 wt% NaOH at 90°C	0.1	—
C_1	Voltage drop for 40 wt% NaOH at 80°C	−1.7087	V
C_2	Voltage drop for 30 wt% NaOH at 70°C	−1.8303	V
C_3	Voltage drop for 50 wt% NaOH at 80°C	−1.3907	V
C_4	Voltage drop for 60 wt% NaOH at 90°C	−1.3202	V
k_1	Correction factor for 40 wt% NaOH at 80°C	0.034	—
k_2	Correction factor for 30 wt% NaOH at 70°C	0.034	—
k_3	Correction factor for 50 wt% NaOH at 80°C	0.03	—
k_4	Correction factor for 60 wt% NaOH at 90°C	0.03	—
l_c,*	Length of the cathode	0.1	m
l_a,*	Length of the anode	0.1	m
ρ_c,*	Resistivity of the cathode	6.9×10^{-7}	Ωm
ρ_a,*	Resistivity of the anode	6.9×10^{-7}	Ωm
R_{mem}*	Resistance of the membrane	0.007×10^{-4}	Ωm^2

*Parameters common to the various experiments: electrolyte concentration, interelectrode gap, and types of electrolyte.

Table 6: Parameters specific to the experiment on interelectrode gap.

Parameters	Description	Value	Unit
d_{am1}	Distance between the anode and the membrane (1 cm)	0.005	m
d_{cm1}	Distance between the cathode and the membrane (1 cm)	0.005	m
d_{am2}	Distance between the anode and the membrane (0.75 cm)	0.00375	m
d_{cm2}	Distance between the cathode and the membrane (0.75 cm)	0.00375	m
d_{am3}	Distance between the anode and the membrane (0.5 cm)	0.0025	m
d_{cm3}	Distance between the cathode and the membrane (0.5 cm)	0.0025	m
d_{am4}	Distance between the anode and the membrane (2 cm)	0.01	m
d_{cm4}	Distance between the cathode and the membrane (2 cm)	0.01	m
ε_1	Void fraction for 1 cm at 80°C	0.22	—
ε_2	Void fraction for 0.75 cm at 80°C	0.22	—
ε_3	Void fraction for 0.5 cm at 80°C	0.32	—
ε_4	Void fraction for 2 cm at 80°C	0.313	—
C_1	Voltage drop for 1 cm at 80°C	−1.2119	V
C_2	Voltage drop for 0.75 cm at 80°C	−1.8646	V
C_3	Voltage drop for 0.5 cm at 80°C	−1.4383	V
C_4	Voltage drop for 2 cm at 80°C	−2.7674	V
k_1	Correction factor for 1 cm at 80°C	0.0294	—
k_2	Correction factor for 0.75 cm at 80°C	0.035	—
k_3	Correction factor for 0.5 cm at 80°C	0.0304	—
k_4	Correction factor for 2 cm at 80°C	0.035	—

Table 7: Parameters specific to the experiment on the types of electrolyte at 40 wt%.

Symbol	Description	Value	Unit
σ_{NaOH1}	σ of NaOH + tap water at 80°C	90.83	S/m
σ_{NaOH2}	σ of NaOH + AC water at 80°C	90.83	S/m
σ_{NaOH3}	σ of NaOH + pressing water at 90°C	108.33	S/m
σ_{NaOH4}	σ of NaOH + factory water at 90°C	108.33	S/m
d_{am}	Distance between the anode and the membrane	0.005	m
d_{cm}	Distance between the cathode and the membrane	0.005	m
ε_1	Void fraction of NaOH + tap water at 80°C	0.2	—
ε_2	Void fraction of NaOH + AC water at 80°C	0.12	—
ε_3	Void fraction of NaOH + pressing water at 90°C	0.35	—
ε_4	Void fraction of NaOH + factory water at 90°C	0.29	—
C_1	Voltage drop for NaOH + tap water at 80°C	−1.7087	V
C_2	Voltage drop for NaOH + AC water at 80°C	−1.5259	V
C_3	Voltage drop for NaOH + pressing water at 90°C	−2.0872	V
C_4	Voltage drop for NaOH + factory water at 90°C	−1.8505	V
k_1	Correction factor for NaOH + tap water at 80°C	0.034	—
k_2	Correction factor for NaOH + AC water at 80°C	0.032	—
k_3	Correction factor for NaOH + pressing water at 90°C	0.033	—
k_4	Correction factor for NaOH + factory water at 90°C	0.033	—

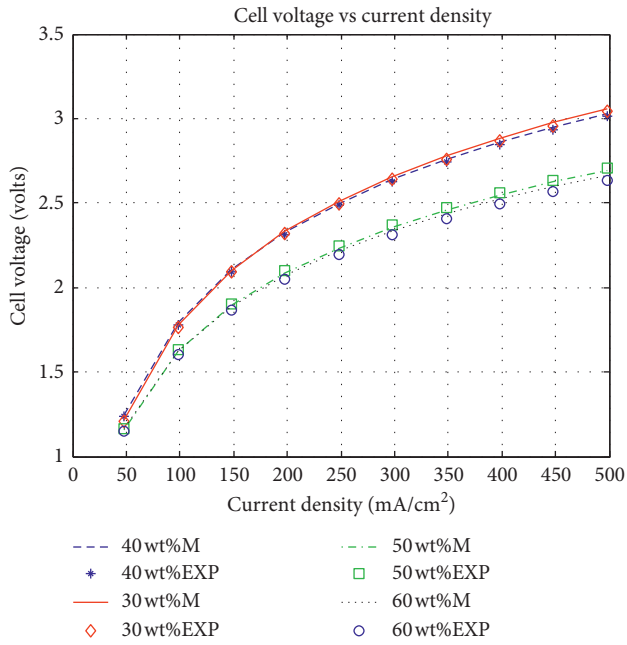

Figure 3: I-V curve for different electrolyte concentrations: M, mathematical model data; EXP, experimental model data.

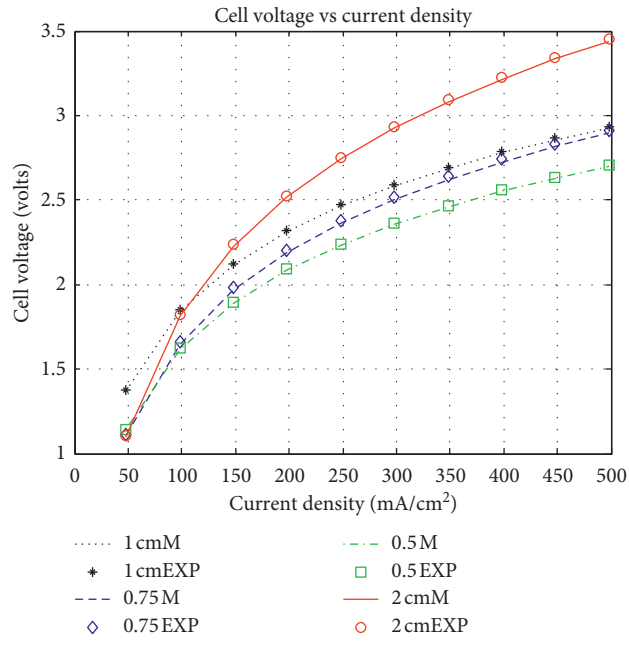

Figure 4: I-V curve for different interelectrode gaps.

values showed that the alkalinity reduced cell voltage. Increasing the alkalinity led to an increase in electrical conductivity which in turn led to an increase in the electrical current passing through the solution and consequently to a decrease of cell voltage.

4.2. Flow Rates for the Different Fluids. Waste water from an AC source, waste water from a pressing, and water from a factory were used and the results were compared with that of a baseline experiment. Values of the hydrogen flow rate were obtained from the experiment with a baseline concentration of 40 wt% NaOH in the various types of liquids. The baseline experiment was that of tap water which is considered neutral.

The flow rate was proportional to the salinity but for the water from pressing which presented an exceptionally low flow rate. It was noticed from simulations performed that water from a pressing had a higher void fraction which meant higher bubbles. This could be the reason for the low flow rate. The water from a factory with a high pH value (11.21) presented the highest flow rate of 12.48×10^{-1} cm^3/min (Figure 6). Slama [32] ranked first ammonia water and urine, with hydrogen flow rates of 11.2 cm^3/min and 11.5 cm^3/min, respectively. The flow rate of urine is about 10 times more than that of the factory water, which could be explained by the large salinity of urine 33.5 g/l [32]

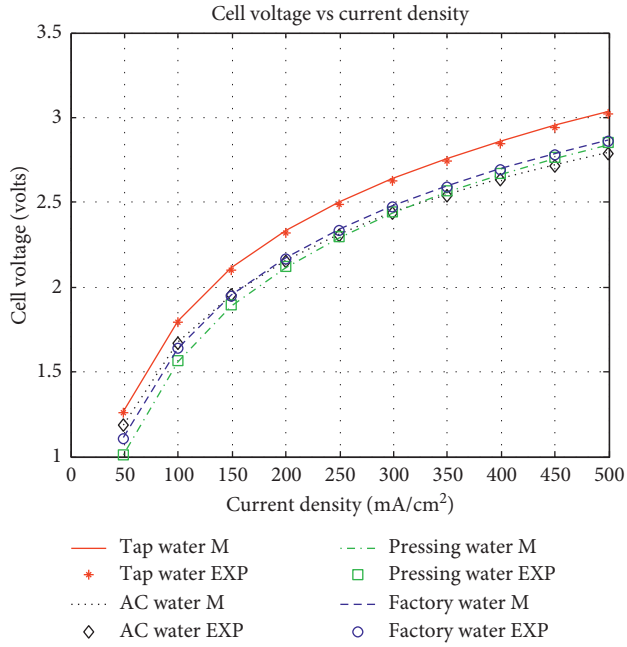

Figure 5: I-V curve for different types of electrolyte.

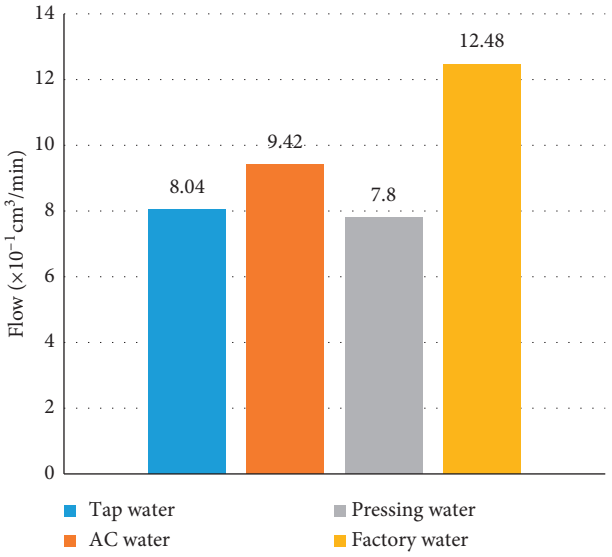

Figure 6: Flow rates of the different types of electrolyte.

compared to that of water from a factory with a salinity of 1.015 g/kg (Table 4). The trend in improving the hydrogen production rate clearly indicated that electrolysis depends not only on the number of ions present in solution but also on their mobility in the solution. Gradual increase in bubbles surely decreased the ion mobility due to hindrance.

The current efficiencies from the above flow rates were calculated and the values showed that the water from the factory had the highest efficiency of about 77.5%, followed by the AC water with 58.7%, and 53.6% for the water from pressing, in absolute terms. The baseline current efficiency for the tap water is 53.4%. Differences in the efficiency could be a result of the variation in current densities due to parasitic losses within the cell. The result of the water from a pressing was slightly higher than that of the tap water, in absolute terms. This could be explained by the fact that the current density is lower in the case of the tap water. Even though the flow rate of tap water was slightly higher than that of the water from a pressing, the current efficiency of water from pressing was relatively higher; this could be due to gas crossover and the bubble effects.

5. Conclusion

This study aimed to determine the electrolyte concentration, interelectrode gap, and the type of electrolyte that can improve the production efficiency of hydrogen through water electrolysis. A multiphysical model was obtained and tested and showed conformity with the mathematical model. In fact, the maximum error is below 2%. Results confirmed that reducing interelectrode gap to 0.5 cm, increasing electrolyte concentration to 60 wt% NaOH, and using electrolytes that provoke less bubbles improved cell performance considerably. Furthermore, the flow rate was greater using the factory water. Water from the dress making factory could be recommended as a suitable electrolyte. In addition, it required moderate cell voltage. Combined effects for the three parameters used in this work should be studied using a factorial design.

Abbreviations

V_{cell}:	Cell voltage
V_{ohm}:	Ohmic overpotential
V_{act}:	Activation overpotential
V_{rev}:	Reversible voltage
T:	Temperature
I:	Current
ΔG:	Gibbs energy
KOH:	Potassium hydroxide
NaOH:	Sodium hydroxide
HHV_{H2}:	Higher heating value of hydrogen
NH_3:	Ammonia
DC:	Direct current
ρ:	Resistivity of electrodes
l:	Length of electrodes
M:	Mathematical
EXP:	Experimental
AWE:	Alkaline water electrolysis
SIMELINT:	Simulation of electrolyzers in intermittent operation
HYDRAC:	Hydrocarbures Analyses Contrôles
FCEVs:	Fuel cell electric vehicles.

Data Availability

The experimental data used to support the findings of this study are provided in Supplementary Materials.

Conflicts of Interest

The authors declare that there are no conflicts of interest regarding the publication of this paper.

Acknowledgments

This work has been successfully completed, thanks to HYDRAC Cameroon that contributed to the standard testing of the electrolyte specimens. The study benefited from the advice of Dr. Anyi Nkongho and thorough comments on the manuscript by Dr. Claude Bakoumé. Chemicals and equipment were provided by the E3M Laboratory of the University of Douala, Cameroon.

Supplementary Materials

Supplementary 1. Appendix A: properties of electrodes [38]. Supplementary 2. Appendix B: data for the conductivity of NaOH. Supplementary 3. Appendix C: measured data and data from plots with the use of Getdata digitizer. (*Supplementary Materials*)

References

[1] N. Muradov and F. Smith, *Local Hydrogen Production via Catalytic Reformation of Fossil and Renewable Feedstock*, Florida Solar Energy Center, Florida Universities Hydrogen Review, Cocoa, FL, USA, 2005.

[2] J. Aicart, *Modélisation et validation expérimentale de la co-électrolyse de la vapeur d'eau et du dioxyde de carbone à haute température*, Ph.D. Thesis, University of Grenoble, Grenoble, France, 2014.

[3] R. D. Bland, T. L. Clarke, and L. B. Harden, "Rapid infusion of sodium bicarbonate and albumin into high-risk premature infants soon after birth: a controlled, prospective trial," *American Journal of Obstetrics and Gynecology*, vol. 124, no. 3, pp. 263–267, 2006.

[4] A. S. Tijani, N. A. B. Yusup, and A. H. A. Rahim, "Mathematical modelling and simulation analysis of advanced alkaline electrolyzer system for hydrogen production," *Procedia Technology*, vol. 15, pp. 798–806, 2014.

[5] E. Dugamin, L. Truche, and F. V. Donzé, "Natural hydrogen exploration guide," *ISRN Geonum-NST*, vol. 1, p. 16, 2019.

[6] I. Abe, "Alkaline water electrolysis," *Journal of the Hydrogen Energy System Society*, vol. 1, pp. 1–21, 1998.

[7] P. M. Chavan, "Hydrogen fuel cell vehicle," *International Journal of Latest Trends in Engineering and Technology*, vol. 7, no. 3, pp. 192–196, 2016.

[8] H. Balat and E. Kırtay, "Hydrogen from biomass-present scenario and future prospects," *International Journal of Hydrogen Energy*, vol. 35, no. 14, pp. 7146–7426, 2010.

[9] I. K. Kapdan and F. Kargi, "Bio-hydrogen production from waste materials," *Enzyme and Microbial Technology*, vol. 38, no. 5, pp. 569–582, 2006.

[10] K. I. Hamada, M. M. Rahman, D. Ramasamy, M. M. Noor, and K. Kadirgama, "Numerical investigation of in cylinder flow characteristics of hydrogen-fuelled internal combustion engine," *Journal of Mechanical Engineering and Sciences*, vol. 10, no. 1, pp. 1792–1802, 2016.

[11] S. Raballo, J. Llera, A. Pérez, and J. C. Bolcich, "Clean hydrogen production in patagonia Argentina," in *Proceedings of the 18th World Hydrogen Energy Conference*, Essen, Germany, May, 2010.

[12] A. Körner, C. Tam, S. Bennett et al., *Technology Roadmap Hydrogen and Fuel Cells*, pp. 1–75, International Energy Agency, Paris, France, 2015.

[13] A. Sohani, S. Naderi, F. Torabi et al., "Application based multi-objective performance optimization of a proton exchange membrane fuel cell," *Journal of Cleaner Production*, vol. 252, p. 119567, 2020.

[14] A. Sohani, S. Naderi, and F. Torabi, "Comprehensive comparative evaluation of different possible optimization scenarios for a polymer electrolyte membrane fuel cell," *Energy Conversion and Management*, vol. 191, pp. 247–260, 2019.

[15] Hydrogen Council, *Path to Hydrogen Competitiveness. A Cost Perspective*, Hydrogen Council, Brussels, Belgium, 2020.

[16] P. E. V. de Miranda, *Science and Engineering of Hydrogen-Based Energy Technologies*, Federal University of Rio de Janeiro, Rio de Janeiro, Brazil, 2019.

[17] M. El-Shafie, S. Kambara, and Y. Hayakawa, "Hydrogen production technologies overview," *Journal of Power and Energy Engineering*, vol. 7, no. 1, pp. 107–154, 2019.

[18] F. Rau, A. Herrmann, H. Krause, D. Fino, and D. Trimis, "Production of hydrogen by autothermal reforming of biogas," *Energy Procedia*, vol. 120, pp. 294–301, 2017.

[19] P. E. Dodds and W. McDowall, *A Review of Hydrogen Production Technologies for Energy System Models*, UCL Energy Institute, University College London, London, UK, 2012.

[20] K. Zouhri and S.-Y. Lee, "Evaluation and optimization of the alkaline water electrolysis ohmic polarization: exergy study," *International Journal of Hydrogen Energy*, vol. 41, no. 18, pp. 7253–7263, 2016.

[21] M. M. Rashid, M. K. Al Mesfer, H. Naseem, and M. Danish, "Hydrogen production by water electrolysis. a review of alkaline water electrolysis, PEM water electrolysis and high temperature water electrolysis," *International Journal of Engineering and Advanced Technology*, vol. 4, no. 3, pp. 80–93, 2015.

[22] Y. Sanath, K. De Silva, P. H. Middleton, and M. Kolhe, "Performance analysis of single cell alkaline electrolyser using mathematical model," *Material Science and Engineering*, vol. 605, p. 012002, 2019.

[23] R. P. Widarningtyas, W. Sulistyo, and W. Widayat, "Potential of hydrogen production through alkaline water electrolysis using solar radiation around Semarang," *E35 Web of Conferences*, vol. 125, no. 3, p. 10006, 2019.

[24] M. Schalenback, A. R. Zeradjanin, O. kasiam, S. Cherevko, and K. J. J. Mayrhofer, "A perspective on low-temperature water electrolysis-challenges in alkaline and acidic technology," *International Journal of Electrochemical Science*, vol. 13, pp. 1173–1226, 2018.

[25] A. prinzhofer, I. Moretti, J. Francollin et al., "Natural hydrogen continuous emission from sedimentary basins: the example of a Brazilian H_2-emitting structure," *International Journal of Hydrogen Energy*, vol. 44, no. 12, pp. 5676–5685, 2019.

[26] T. Zhou and B. Francois, "Modeling and control design of hydrogen production process for an active hydrogen/wind hybrid power system," *International Journal of Hydrogen Energy*, vol. 34, no. 1, pp. 21–30, 2009.

[27] O. Ulleberg, "Modeling of advanced alkaline electrolyzers: a system simulation approach," *International Journal of Hydrogen Energy*, vol. 28, no. 1, pp. 21–33, 2003.

[28] W. Hug, H. Bussmann, and A. Brinner, "Intermittent operation and operation modeling of an alkaline electrolyzer," *International Journal of Hydrogen Energy*, vol. 18, no. 12, pp. 973–977, 1993.

[29] Y. S. K. De Silva and P. H. Middleton, "Design of an alkaline electrolysis stack," M.Sc. Thesis, University of Agder, Faculty

of Engineering and Science, Department of Engineering Sciences, Kristiansand, Norway, 2017.
[30] A. N. Colli and H. H. Girault, "Compact and general strategy for solving current and potential distribution in electrochemical cells composed of massive monopolar and bipolar electrodes," *Journal of the Electrochemcal Society*, vol. 164, no. 11, pp. 3465–3472, 2017.
[31] A. N. Colli and J. M. Bisang, "Current and potential distribution in electrochemical reactors with activated or resistive electrodes. a multiregion and open source approach," *Electrochimica Acta*, vol. 290, pp. 676–685, 2018.
[32] R. B. Slama, "Production of hydrogen by electrolysis of water: effects of the electrolyte type on the electrolysis performances," *Computational Water, Energy, and Environmental Engineering*, vol. 2, no. 2, pp. 54–58, 2013.
[33] A. Rashed and A. Elmaihy, "Theoretical and experimental performance of oxy-hydrogen generators," *Arabian Journal for Science and Engineering*, vol. 43, pp. 1279–1289, 2018.
[34] A. valente, D. Iribarren, and J. Dufour, "End of life of fuel cells and hydrogen products: from technology to strategies," *International Journal of Hydrogen Energy*, vol. 44, no. 38, pp. 20965–20977, 2019.
[35] S. Licht, S. Liu, B. Cui et al., "Comparison of alternative molten electrolytes for water splitting to generate hydrogen fuel," *Journal of the Electrochemical Society*, vol. 163, no. 10, pp. 1162–1168.
[36] A. N. colli, H. H. H. Girault, and A. Battistel, "Non-precious electrodes for practical alkaline water electrolysis," *Materials*, vol. 12, no. 1336, pp. 2–17, 2019.
[37] D. Martinez and R. Zamora, "MATLAB simscape model of an alkaline electrolyser and its simulation with a directly coupled PV module," *International Journal of Renewable Energy Research*, vol. 8, no. 1, pp. 552–560, 2018.
[38] C. C. H. Diaz, *Modélisation Multi-Physique et Électrique d'un Électrolyseur Alcalin*, Library and Archives Canada, Ottawa, Canada, 2011.
[39] M. S. Opu, "Effect of operating parameters on performance of alkaline water electrolysis," *Interntional Journal of Thermal and Environmental Engineering*, vol. 9, pp. 53–60, 2015.
[40] N. Never, *Air Pollution Control Engineering*, McGraw-Hill, Singapore, 1995.
[41] T. Godish, *Air Quality*, Lewis Publishers, Boca Raton, FL, USA, 1991.
[42] E. R. Cohen and B. N. Taylor, "Fundamental physics constants," *Journal of Research of National Bureau of Standards*, vol. 92, no. 2, pp. 85–95, 1987.
[43] G. Chisholm and L. Cronin, *Hydrogen from Water Electrolysis*, pp. 315–343, School of Chemistry, University of Glasgow, Glasgow, UK, 2016.
[44] A. J. McEvoy, "Fundamentals and applications of electrochemistry," *ChemInform*, vol. 45, no. 26, p. 01018, 2013.
[45] F. Hine, *Electrode Processes and Electrochemical Engineering*, p. 75, Plenum Press, New york, NY, USA, 1985.
[46] A. Angulo, P. V. der Linde, H. Gardeniers, M. Modestino, and D. F. Rivas, "Influence of bubbles on the energy conversion efficiency of electrochemical reactors," *Joule*, vol. 4, no. 3, pp. 555–579, 2020.
[47] D. Lumanauw, "Hydrogen bubble characterization in alkaline water electrolysis," M.Sc. Thesis , University of Toronto, Toronto, Canada, 2000.
[48] R. E. De La Rue and C. W. Tobias, "On the conductivity of dispersions," *Journal of the Electrochemical Society*, vol. 106, no. 9, pp. 827–833, 1959.